

International Journal of  
**Applied  
Ceramic  
TECHNOLOGY**

Ceramic Product Development and Commercialization

## **Fluorhydroxyapatite Coatings Obtained by Flame-Spraying Deposition**

**Réka Barabás,\* Erzsébet Sára Bogya, Valentina Roxana Dejeu, and Liliana Bizo**

*Department of Chemical Engineering and Oxide Materials Science, Babeş-Bolyai University,  
Cluj-Napoca 400028, Romania*

**Christos G. Aneziris and Tim Kratschmer**

*Institute of Ceramic, Glass and Construction Materials, Technical University of Freiberg, Freiberg  
09599, Germany*

**Patrik Schmutz**

*Swiss Federal Laboratories for Materials Testing and Research (EMPA), Laboratory for Corrosion and  
Materials Integrity, CH-8600 Dübendorf, Switzerland*

---

Medical-grade hydroxyapatite has been used in different forms and has been applied in different ways. To improve the thermal properties of hydroxyapatites, samples with precise fluoride content were prepared (fluorhydroxyapatites) to avoid the toxic effect of the higher amount of fluoride in the organism. Plasma spraying is the most common of all the application techniques used in the coating processes of hydroxyapatite, even though the partial decomposition of hydroxyapatite was reported. To avoid this inconvenience, another method was used for coating: flame spraying. This technology is a novelty regarding the fluorhydroxyapatite coatings on metallic surfaces. Its positive results present a new, cheap, and efficient possibility for fluorhydroxyapatite coatings on metallic implants.

The stabilizing effect of fluoride was confirmed by the results obtained for the coating characterization, which shows the presence of a single phase: fluorhydroxyapatite.

## Introduction

Hydroxyapatite  $\text{Ca}_{10}(\text{PO}_4)_6(\text{OH})_2$  (symbolized here as HAP) is a major component of the bone and teeth material, thus having the necessary and desired properties for being biocompatible. Because of this fact, many researchers have focused their studies for using them as bone and/or tooth implants or substitutions.<sup>1–5</sup> The advantages of using hydroxyapatites as biomaterials are incontestable: biocompatibility, osteoconductivity, and bioactivity. Despite these advantages, there are some deficiencies: low mechanical resistance, poor thermal, and chemical stability during long-term contact with biological fluids/tissues. Although HAP layers deposited on implants showed good fixing performance after implantation, long-term exposure to biological fluids led to degradation, because of the dissolution of hydroxyapatite.<sup>6</sup> By partial substitution of  $\text{OH}^-$  groups by  $\text{F}^-$  ions results the formation of fluoridated hydroxyapatites,<sup>7,8</sup> which have lower solubility than HAP, promote bioactivity, and exhibit better thermal stability. Because fluorine in high quantities and during long-term action has a noxious effect, the fluorine content of fluorhydroxyapatites ( $\text{Ca}_{10}(\text{PO}_4)_6(\text{OH})_{2-x}\text{F}_x$ ) has been limited to  $0.67 < x < 1.48$ .<sup>9</sup> The fluoride content and quantity present in the lattice are the factors that improve the *thermal* and *chemical* stability of these apatites.<sup>6</sup> Fluorine improves the bioactive properties too; it increases osteoconductivity and the regeneration rate of the near-by cells.<sup>10</sup> Although FHAP is not considered a biomaterial, in the range mentioned above, it could be qualified as a biomaterial with substantial applications in medicine.

Flame spraying is part of a wider group of coating processes known as thermal spraying. A wide variety

of materials can be deposited as coatings using this process and the vast majority of components are sprayed manually.

The most widely used alloys for implants are those based on titanium, which present good results but are very expensive. An alternative is the deposition on magnesium alloys; they appear to be potentially biodegradable and biocompatible materials. In recent years, there has been an increasing interest in magnesium and magnesium alloys as degradable metal implants used in orthopedic surgery. Magnesium and magnesium alloys have many outstanding advantages, which have similar mechanical properties to natural bone and can degrade in the physiological environment through electrochemical corrosion.<sup>11–13</sup>

The reason why flame spraying could be a good alternative among other surface engineering techniques is that it offers the easiest and most tolerable working conditions, low costs, and the required coating performance. Flame spraying has distinct advantages, including lower flame temperature (approximately maximum  $3000^\circ\text{C}$ ) compared with other spraying processes (e.g., by plasma spraying, the high temperature ( $10,000^\circ\text{C}$ ) leads to thermal decomposition).<sup>14,15</sup> These benefits contribute to the expansive usage of the process.

In this process, the sprayed materials could be powders, wires, or ceramic rods. A better coating quality was obtained using wires or rods and not powders.<sup>16</sup> The coatings were made with a gun similar to a wire gun (Fig. 1). The principle of the operation in either gun is similar—the nozzle's flame is concentric to the wire or rod in order to maximize uniform heating. In the process, the ceramic rod material is completely melted us-

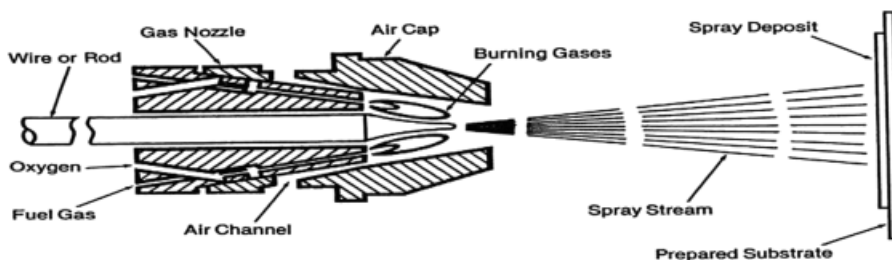


Fig. 1. Flame spraying process.

ing the heat from the combustion of a fuel gas (usually acetylene or propane) with oxygen. Rod flame-spraying process produces coatings of high levels of density and adhesion.<sup>14</sup>

The objectives of this work were to improve the thermal stability of hydroxyapatite by partial substitution of OH<sup>-</sup> groups with fluoride ions and to find a new alternative and efficient technology for the deposition of fluorhydroxyapatite coatings.

## Experimental Procedure

### Preparation

Fluorhydroxyapatite ( $\text{Ca}_{10}(\text{PO}_4)_6(\text{OH})_{2-x}\text{F}_x$ ,  $x = 1$ ) was prepared using a procedure similar to that reported for the preparation of hydroxyapatite:  $\text{Ca}_{10}(\text{PO}_4)_6(\text{OH})_2$ .<sup>10</sup> The reaction vessel (with hydraulic closing and an ascending refrigerator) was a 2000-cm<sup>3</sup> glass flask. Analytical-grade  $\text{Ca}(\text{NO}_3)_2 \cdot 4\text{H}_2\text{O}$ ,  $(\text{NH}_4)_2\text{HPO}_4$ , and  $\text{NH}_4\text{F}$  reagents were used to prepare stock solutions. 870 cm<sup>3</sup> of  $\text{Ca}(\text{NO}_3)_2$  stock solution (0.5M) was transferred into the flask. The temperature was raised to 50°C and finally 950 cm<sup>3</sup>  $(\text{NH}_4)_2\text{HPO}_4$  solution (0.3M) (containing 3.14–1.05 g  $\text{NH}_4\text{F}$ ) was added in drops to the  $\text{Ca}(\text{NO}_3)_2$  solution. The pH was adjusted to 9–9.5 pH using concentrated  $\text{NH}_4\text{OH}$  solution. The flask was placed in a thermo-stated shaker, which allowed intensive mixing of the solution and the precipitate. After the desired stirring time, the precipitate was filtered, thoroughly washed, and dried at 105°C for 10 h. The resulting compact material was ground in an agate mill, and then fired at 1000°C for 1 h.<sup>17</sup>

### Rod Production and Spray Parameters

To feed the flame-spraying gun with rods, the raw materials were mixed in advance with a thermoplastic injection moulding binder (Siliplast HO, Zschimmer & Schwarz, Koblenz, Germany) and extruded in a heatable twin-screw extruder from BrabenderR OHG (Duisburg, Germany).

The extruded rods (Fig. 2) were thermally treated with adjacent sintering at 1100°C for 2 h. The diameter of the rods after sintering had to be between 6.0 and 6.2 mm to fit the flame-spray gun.

Table I presents the parameters of the flame-spraying process. A MasterJet flame-spray gun (RokideR Spray Unit, Saint-Gobain, Avignon, France) was used.



Fig. 2. Ceramic rods used for flame spraying.

### Characterization Methods

The prepared material was characterized by different physical–chemical methods:

- *Infrared (IR) spectroscopy*: The material was characterized by IR spectroscopy (in KBr pellets) using a Jasco FT/IR-615 spectrophotometer (Easton, MD).
- *Scanning electron microscopy (SEM)*: The general structure of the material was determined using a scanning electron microscope, Philips XL30 ESEM-FEG (Eindhoven, The Netherlands), by coating them with a thin layer of gold.
- *X-ray diffraction (XRD) measurements*: The samples morphology and crystallinity were studied by X-ray measurements using a Shimadzu XRD-6000 apparatus. Scans were conducted from 10° to 80° modifying the angle by 2° each step.
- *Particle size analysis* in suspension was made using a Coulter Counter micro- and nanoparticle analyzer, Shimadzu SALD-7101 (Tokyo, Japan).
- *The calcium and phosphor content* of samples were determined using an inductively coupled plasma

Table I. Parameters of the Spray Process (nm<sup>3</sup>/h, norm cubic meters per hour)

Flow of oxygen gas	3.5 (nm <sup>3</sup> /h)
Flow of acetylene gas	0.8 (nm <sup>3</sup> /h)
Flow of air	28 (nm <sup>3</sup> /h)
Gun-to-substrate distance	100 (mm)
Rod feed rate	10 (mm/min)

emission spectrometer; the measurements were carried out using an ICP-OES BAIRD 2070 type apparatus.

- *The fluoride content* of the samples was determined using a fluoride-selective electrode. The pF values were obtained with a F500 fluoride-selective electrode connected to a pH/ion Analyzer Orion Model 901 against a saturated Ag/AgCl electrode (Wissenschaftlich-Technische Werkstätten, Weilheim, Germany).

## Results and Discussion

### Powder Characterization

*SEM:* The SEM micrograph (Fig. 3a) of the calcinated fluorhydroxyapatite powder shows that the individual particles have an average size of  $0.25\ \mu\text{m}$  (in accordance with the results given by Coulter Counter). Because of the sintering at  $1000^\circ\text{C}$ , the single particles stick together. The micrograph at a lower resolution (Fig. 3b) presents the high agglomeration tendency of the sintered powder.

*Particle Size Analysis:* Particle size distribution (Fig. 4) shows that 23% of the particle amount was in the range of  $0.1\text{--}0.5\ \mu\text{m}$  (single particles) and 77% was in the range of  $0.5\text{--}10\ \mu\text{m}$  (agglomerated particles).

Based on preliminary experiments, it is known that in order to obtain a uniform coating the mean diameter of the particles must be in the range of  $1\text{--}5\ \mu\text{m}$ .

*IR Spectroscopy:* According to the facts presented by R. I. Martin and P. W. Brown, if the precipitation of fluorhydroxyapatites is accomplished at higher concen-

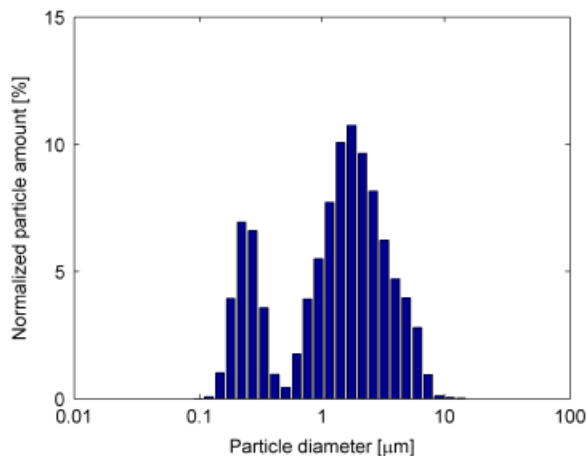


Fig. 4. Particle size distribution of fluorhydroxyapatite made with a Coulter Coulter.

trations than  $0.75 \cdot 10^{-3}\text{M}$  fluorine, the coexistent phases at equilibrium contain fluorhydroxyapatite and  $\text{CaF}_2$ .<sup>18</sup>

As described previously in the *Preparation* section, the precipitation was accomplished at higher fluorine concentrations ( $x = 1$ ). The IR spectra (Fig. 5.) show that the FHAP spectrum is similar to fluorapatite (FAP). In a recent study, it was reported that between HAP and FAP spectra exists a marked difference: the absence of the peak at  $633\ \text{cm}^{-1}$  (corresponding to the  $\text{OH}^-$  groups) and that the spectra of different FHAP ( $x = 1, 1.48$ ) depend on the fluoride content; at a small amount of fluorine ( $x = 0.67$ ), the peak at  $633\ \text{cm}^{-1}$  is still visible. By increasing the fluorine content, this peak disappears.

*Chemical Analysis (Calcium, Phosphor, and Fluorine Content):* In Table II are presented the values of the Ca and

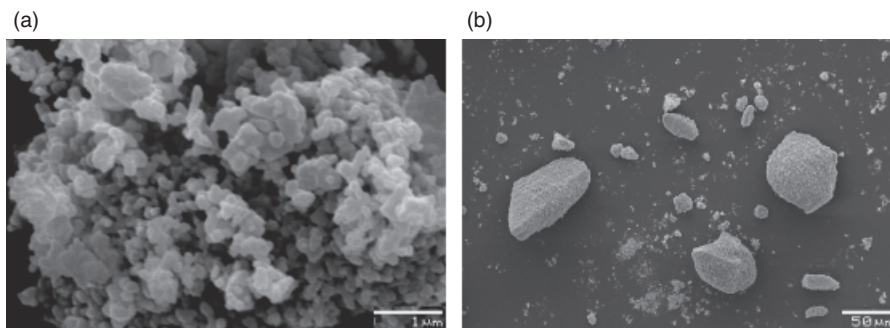


Fig. 3. Scanning electron microscopy photomicrographs of calcinated FHAP powder at (a)  $\times 20,000$ , magnification and (b)  $\times 300$ , magnification.

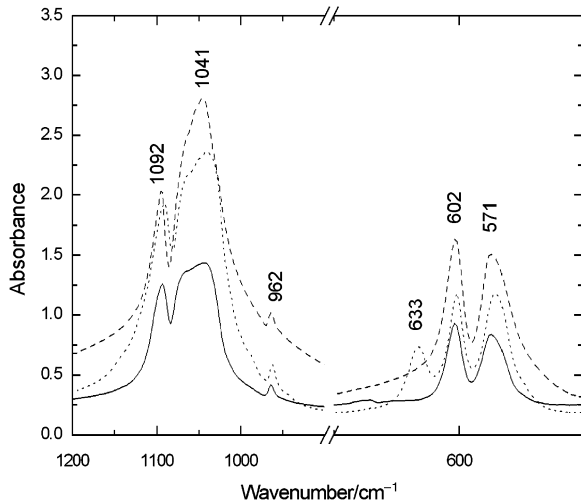


Fig. 5. Infrared spectra of calcined hydroxyapatite (···), calcined fluorapatite (—), and calcined fluorhydroxyapatite (—).

P content as well as their ratio Ca/P, carried out by ICP. The values obtained show that the resulting apatites were stoichiometric, the Ca/P ratio was very close to the theoretical ratio  $\text{Ca/P} = 1.67$ . The lack of secondary phases in the diffractograms confirms the stoichiometric character of the samples. Table II also presents data referring to the fluorine content of the prepared FHAP. The ratio between the initial fluorine quantity introduced in the reaction and the fluorine content of the products indicates the degree of transformation of fluorine during this process.

### Ceramic Rod Characterization

**XRD:** The XRD spectra (Fig. 6) show no major differences among powder, rod, and coating. All of them present good crystallinity due to the very sharp peaks observed. The preparation procedure of the rod did not change the FHAP structure. Peaks from the coating and the Mg alloy substrate (noted by stars in the figure) were observed. Based on the XRD results, it was

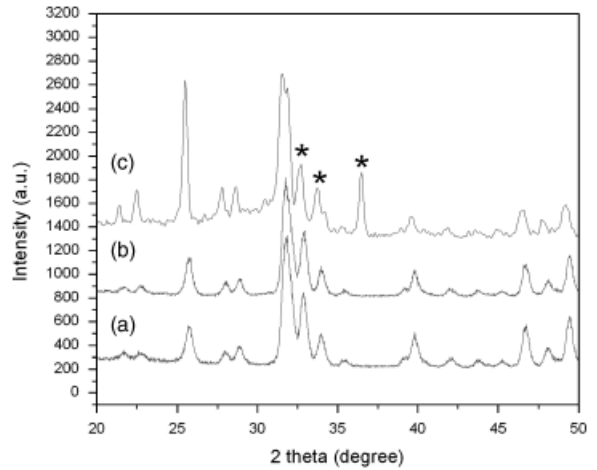


Fig. 6. X-ray diffraction patterns of fluorhydroxyapatite powder (a), rod (b), and coating deposited on an Mg alloy substrate (c).

difficult to judge if the other peaks of fluorhydroxyapatite appeared because they might be covered with the peaks of the substrate. Apart from the substrate peaks, it could be stated that all XRD peaks of the coatings can be ascribed to apatite. No other impurity phases such as CaO,  $\beta$ -TCP, or  $\text{CaF}_2$  were detected (FHAP patterns indicated that a single-phase FHAP was formed).

### Coating Characterization

In this work, FHAP deposition was made on a magnesium alloy with the following chemical composition: 96.32% Mg, 2.51% Al, 0.36% Mn, 0.77% Zn, and 0.05% of other elements such as Zr, Cu, Si, Fe, Ni, Ca, Sn, Be, and Pb.

### SEM

The agreed optimum coating thickness is 50–100  $\mu\text{m}$ <sup>19,20</sup>; this thickness influences coating adhesion and fixation. The measured thickness of the layer

Table II. Theoretical and Measured Ca, P, and F Content of HAP and FHAP

Sample	$\text{Ca}_{\text{theoretic}}$ (wt%)	$\text{Ca}_{\text{measured}}$ (wt%)	$\text{P}_{\text{theoretic}}$ (wt%)	$\text{P}_{\text{measured}}$ (wt%)	Ca/ P	$\text{F}_{\text{theoretic}}$ (wt%)	$\text{F}_{\text{measured}}$ (wt%)	$\frac{\text{F}_m}{\text{F}_t} \times 100\%$
HAP	39.84	39.74	18.52	18.5	1.66	—	—	—
FHAP	39.76	39.47	18.48	18.46	1.65	1.88	1.52	81.11

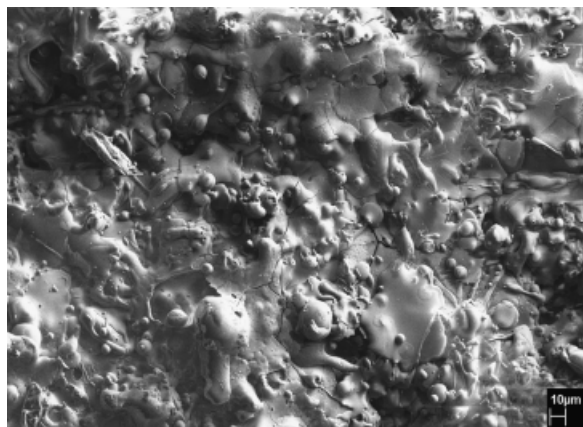


Fig. 7. Scanning electron microscopic photomicrograph ( $\times 300$ , magnification) of fluorhydroxyapatite coating on magnesium alloy.

obtained by flame spraying was  $50 \pm 10 \mu\text{m}$ . A common effect during flame-spraying processes is the tensions that appear in the cooling process, which could be observed in Fig. 7. Another effect is the inequable melting of the particles; the bubbles that are observed in Fig. 7 are particles that did not melt. This issue could be avoided using fluorhydroxyapatite with uniform particle size distribution, preferably nanoparticles. In the future, the coating process needs to be optimized in order to obtain a uniform thickness of the layer on the implant surface.

## Conclusions

Although *plasma spraying* is well known and widely used, it still presents certain disadvantages like the thermal decomposition of the material during the deposition and the high costs of the process. In this paper, the authors suggest a new method with lower costs and a lower work temperature: *flame spraying*. Thermal properties were also improved by adding fluoride in the material preparation. *Flame-spraying technique* proves to be an adequate and promising method to obtain biomaterial coatings on implants. The deposition technology consists of two stages: 1—rod fabrication and 2—material deposition on the metallic support. Definitely, there are certain difficulties: each material has its own technology for rods fabrication. In this work, the authors succeed in establishing the optimum technology

for the fabrication of *FHAP* rods. Further experiments are needed in order to optimize the flame-spraying process to obtain coatings with the required quality for biomedical applications.

## References

1. J. W. Nicholson, *Chemistry of Medical and Dental Materials*, Vol. 85. The Royal Society of Chemistry, London, 2002.
2. M. Shirkhazadeh and M. Azadegan, "Formation of Carbonate Apatite on Calcium Phosphate Coatings Containing Silver Ions," *J. Mater. Sci.: Mater. Med.*, 9 [7] 385–391 (1998).
3. Ts. De Araujo, Zs. Macedo, De O. Pasc, and V. Meg, "Production and Characterization of Pure and  $\text{Cr}^{3+}$ -Doped Hydroxyapatite for Biomedical Applications as Fluorescent Probes," *J. Mater. Sci.*, 42 [7] 2236–2243 (2007).
4. A. Bandyopadhyay, E. A. Withey, J. Moore, and S. Bose, "Influence of ZnO Doping in Calcium Phosphate Ceramics," *Mater. Sci. Eng. C, Biomim. Supramol. Syst.*, 27 [1] 14–17 (2007).
5. S. J. Kalita and H. A. Bhatt, "Nanocrystalline Hydroxyapatite Doped With Magnesium and Zinc: Synthesis and Characterization," *Mater. Sci. Eng. C-Biomim. Supramol. Sys.*, 27 [4] 837–848 (2007).
6. K. Cheng, S. Zhang, W. Weng, and X. Zeng, "The Interfacial Study of Sol-Gel-Derived Fluoridated Hydroxyapatite Coatings," *Surf. Coat. Technol.*, 198 [1–3] 242–246 (2005).
7. R. Fabian, I. Kotsis, P. Zimany, and P. Halmos, "Preparation and Chemical Characterization of High Purity Fluorapatite," *Talanta*, 46 1273–1277 (1998).
8. R. Fabian, I. Kotsis, and Z. Pilter, "Comparison of Properties of Fluorapatites Prepared by Solid State Reaction and Precipitation," *Hung. J. Ind. Chem.*, 27 [4] 259–263 (1999).
9. K. Cheng, W. Weng, H. Wang, and S. Zhang, "In Vitro Behavior of Osteoblast-Like Cells on Fluoridated Hydroxyapatite Coatings," *Biomaterials*, 26 6288–6295 (2005).
10. R. Barabás, A. Pop, E. Fazakas, and V. Dejeu, "Comparative Analyses of Fluorapatite and Biomedical Fluorhydroxyapatites Prepared by Precipitation and Solid State Reaction," *Proceedings of the 10th ECerS Conference*, Berlin, Götter Verlag, 925–930, (2007).
11. Y. Jing-Xin, J. Yan-Peng, Y. Qing-Shui, Z. Yu, and Z. Tao, "Calcium Phosphate Coating on Magnesium Alloy by Biomimetic Method: Investigation of Morphology, Composition and Formation Process," *Front. Mater. Sci. China*, 2 [2] 149–155 (2008).
12. M. P. Staiger, A. M. Pietak, J. Huadmai, and G. Dias, "Magnesium and its Alloys as Orthopedic Biomaterials: A Review," *Biomaterials*, 27 1728–1734 (2006).
13. A. Pietak, P. Mahoney, and G. J. Dias, "Bone-Like Matrix Formation on Magnesium and Magnesium Alloys," *J. Mater. Sci.: Mater. Med.*, 19 407–415 (2008).
14. E. Lugscheider, "Handbuch der thermischen Spritztechnik," DVS Media, 21–23, 2002
15. R. Z. LeGeros, J. P. LeGeros, Y. Kim, R. Kijkowska, R. Zheng, C. Bautista, and J. L. Wong, "Calcium Phosphates in Plasma-Sprayed HA Coatings," *Ceram. Transac.*, 48 173–189 (1995).
16. Fr.-W. Bach and Th. Duda, *Moderne Beschichtungsverfahren*, Wiley-VCH Verlag, Berlin, Germany, (2005).
17. R. Fabian (Barabás), and I. Kotsis, "Comparison of Properties of Fluorapatites Prepared by Solid State Reaction and Precipitation," *Hung. J. Ind. Chem.*, 27 259–263 (1999).
18. R. I. Martin and P. W. Brown, "Effects of Sodium Fluoride, Potassium Fluoride and Ammonium Fluoride Solutions on the Hydrolysis of  $\text{CaHPO}_4$  at  $37.4^\circ\text{C}$ ," *J. Cryst. Growth*, 183 [3] 417–426 (1998).
19. B. D. Ratner, A. S. Hoffman, F. J. Schoen, and J. E. Lemons, *Biomaterials Science: An Introduction to Materials in Medicine*, 2nd edition, Elsevier, San Diego, CA, 162–170, 2004.
20. S. Gottschling, R. Kohl, A. Engel, and H. J. Oel, "Characterization of Plasma Sprayed Hydroxyapatite Coatings on Titanium Toothroot Implants," *Bioce-ram.: Mater. Appl.*, 48 201–213 (1995).